

## Characterization of Sintered NdFeB Magnets after Phosphating in Alkaline and Acidic Environments

Saliba-Silva, A.M.<sup>1</sup>; de Melo, H.G.<sup>2</sup>; Baker, M.A.<sup>3</sup>; Brown, A.M.<sup>3</sup>; Costa, I.<sup>1</sup>

<sup>1</sup> Instituto de Pesquisas Energeticas e Nucleares, IPEN/CNEN-SP

Caixa Postal 11049, CEP 05422-970, São Paulo-SP e-mail : adonis@net.ipen.br

<sup>2</sup> EPUSP - Departamento de Engenharia Química, SP, Brasil.

<sup>3</sup> School of Mechanical and Materials Engineering, University of Surrey, Guildford, UK

**Keywords:** Corrosion; EIS, Sintered Magnets; Surface Analysis; Phosphating.

**Abstract:** Despite their excellent magnetic properties NdFeB permanent magnets are highly susceptible to corrosion. Conversion coatings, such as phosphating, have been evaluated as promising methods for corrosion control of these types of magnets. In the present work, alkaline and acid solutions have been used for phosphating a NdFeB commercial magnet. Characterization of the phosphate layer formed in alkaline solution ( $\text{pH} > 8$ ) of  $\text{Na}_2\text{HPO}_4$ , was carried out by Auger Electron Spectroscopy (AES), Energy Dispersive X-ray analysis (EDX), and Electrochemical Impedance Spectroscopy (EIS). AES and EIS results showed that the layer formed in the alkaline solution was not protective. On the other hand, the phosphate layer formed in the acid solution ( $3,8 < \text{pH} < 4,6$ ) of  $\text{NaH}_2\text{PO}_4$  produced a significant increase in the magnet corrosion resistance. It is proposed that improvement in the corrosion resistance of the magnet phosphated in the acid solution was due to a more uniform attack of the whole surface leading to the formation of a more continuous and protective conversion layer, compared to that formed in alkaline solution. The resistance of the conversion coating layer formed in acidic medium, estimated from EIS data, is in-between  $5000$  and  $20000 \Omega \text{ cm}^2$ , while that of the layer formed in the alkaline environment is less than  $1000 \Omega \text{ cm}^2$ . It is believed that precipitation of phosphates at high pH's do not produce a homogeneous coverage of the various phases of sintered NdFeB magnets, since the precipitation is favored at the more active areas of the magnet.

### Introduction

NdFeB permanent magnets produced by Powder Metallurgy (P/M) are largely used in the electronic industry. They are well known for their excellent magnetic properties and are increasingly substituting Sm-Co magnets mainly due to their lower cost and improved magnetic properties for low temperature applications. Sintered  $\text{Nd}_2\text{Fe}_{14}\text{B}$  is mainly used in one particular application, the production of voice coil motors (VCM) of hard disk drives (HDD), which consumes about 60% of the current production [1].

NdFeB magnets have low corrosion resistance in various working environments [2-7], limiting their field of application [8]. To overcome this drawback, they are usually protected by coatings. Most of the published literature concerning coatings on sintered NdFeB magnets refers to organic and metallic coatings [9-12], with no concern about the role of surface pretreatment on the corrosion performance of the coated material. Only recently, has phosphating been studied as a possible pre-treatment to increase both, the corrosion resistance of the magnet [13-15] and the adherence of the coating to the substrate. Phosphating has no significant effect on magnetic properties, or dimension of magnets, as very thin layers, below  $1 \mu\text{m}$ , are formed. Moreover, the

presence of the conversion coating can improve the corrosion performance of the magnet by acting as an intermediate layer at defective areas of the coatings.

In this study, the effect of composition of the phosphating solution on the corrosion resistance of a commercial sintered NdFeB magnet has been investigated. Two solutions of different pH's, one acid and another alkaline, were used. The two main phases of the magnet (Nd-rich and  $\phi$ -phase) have been analyzed by Auger Electron Spectroscopy and Energy Dispersive X-ray Analysis (EDX) to evaluate the phosphate layer coverage. Electrochemical Impedance Spectroscopy (EIS) has been used to examine the corrosion resistance of the phosphated magnets and to compare the corrosion characteristics of the phosphate layer obtained in both acid and basic solutions.

### Material and Methods

*Material:* A commercial sintered NdFeB magnet produced by Crucible – U.S.A., whose composition is given elsewhere [18], was used in this investigation.

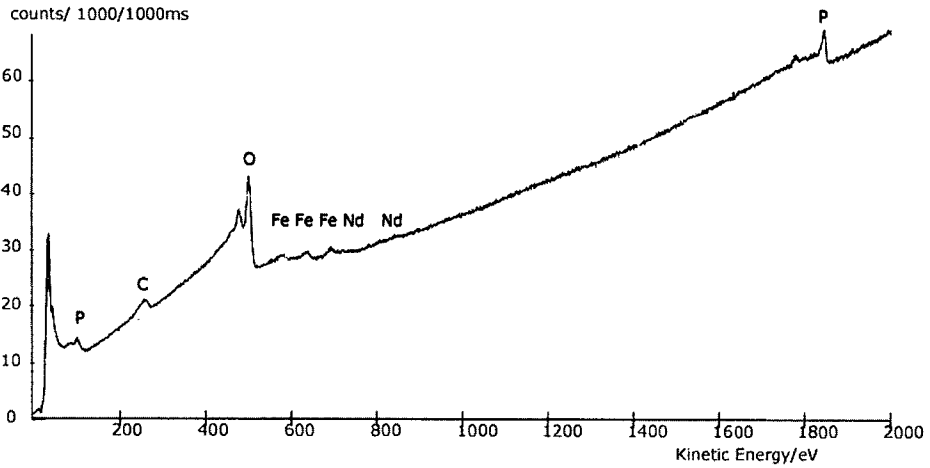
*Specimen preparation:* Electrodes with an area of approximately  $1.3 \text{ cm}^2$  were prepared by cold resin mounting. The surface was prepared by grinding with silicon carbide paper up to grade #1000, followed by degreasing with acetone, using an ultrasonic bath, and drying under a hot air stream.

*Experimental set-up:* A three electrode cell arrangement was used for the electrochemical measurements, with a graphite rod and a saturated calomel electrode (SCE) as counter and reference electrodes, respectively. EIS measurements were accomplished with a 1255 Solartron frequency response analyzer coupled to a EG&G 273A Potentiostat. All measurements were performed in potentiostatic mode and at the corrosion potential,  $E_{\text{corr}}$ . Before performing EIS experiments, the magnet specimens were immersed for 24 hours in either of the two phosphating solutions: 0.15 M  $\text{NaH}_2\text{PO}_4$  solution (pH=4.6) [solution 1] or 0.15 M  $\text{NaH}_2\text{PO}_4$  (pH=9.3) [solution 2], in order to produce the conversion coating. The corrosion resistance of the phosphated magnets was then investigated by EIS in a 0.01M  $\text{Na}_2\text{SO}_4$  test solution. For comparison, EIS experiments were also performed with untreated magnets in the same test solution. The amplitude of the perturbation signal was 10 mV, and the frequency range studied from  $10^5$  to  $10^{-2}$  Hz. The solutions were all quiescent, aerated and at a temperature of  $(20 \pm 2)^\circ\text{C}$ .

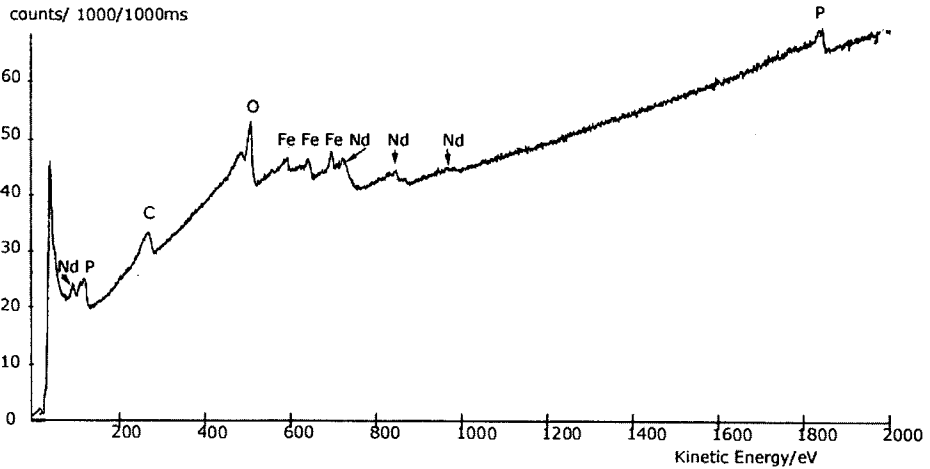
*AES/EDX/SEM analysis:* Scanning electron microscopy and chemical analysis (AES and EDX) of the phosphate layers formed by immersion in acid or basic solutions for 24 hours was carried out using a VG Microlab mk II onto which an EDX detector had been mounted. AES/EDX point spectra were acquired using an electron beam operating at 15 keV and specimen current of 10-15 nA. The Auger spectra were acquired at a Constant Retard Ratio (CRR) of 4, step of 1 eV, for general wide scans and CRR 10, step 0.3 eV, for the phosphorous KLL peak.

### Results and Discussion

SEM and chemical analysis reveal that the magnet develops different conversion coating layer morphologies and compositions depending on the phosphating solution used. Figure 1 shows the Auger spectra of the phosphated magnet in acid solution. Nd, Fe, O and P peaks are present in the spectra from both the Nd-rich phase (Fig 1 (a)) and  $\phi$ -phase (Fig. 1 (b)). (The C peak originates from overlayer hydrocarbon contamination.). A strong P peak was also found in the EDX spectra from both phases, indicating the presence of a phosphate layer covering the entire surface [15].



(a)



(b)

**Fig. 1.** Auger spectra of Nd rich-phase and  $\phi$ -phase phosphated in solution of 0.15M  $\text{NaH}_2\text{PO}_4$  (pH=4.6): (a)  $\phi$ -phase; (b) Nd rich phase.

For the  $\phi$ -phase a higher energy resolution scan showed the position of P  $\text{KL}_{23}\text{L}_{23}$  peak to be 1851 eV, typical of a phosphate and in good agreement with that obtained for iron phosphate at 1850.5 eV [16]. The presence of the strong Fe  $\text{L}_{3\text{MM}}$  triplet between 570 and 700 eV and lower intensity Nd  $\text{N}_{5}\text{M}_{45}\text{M}_{45}$  and  $\text{N}_{45}\text{M}_{45}\text{N}_{67}$  peaks at 733 and 840 eV respectively, indicate the  $\phi$ -phase phosphate to have a high Fe/Nd ratio. The Nd-rich phase exhibits much stronger Nd MNN peaks, clearly representative of a lower Fe/Nd ratio.

The P  $\text{KL}_{23}\text{L}_{23}$  peak for the Nd-rich phase is composed of two components, the low energy component corresponding to a phosphate, the peak position being 1848 eV, and a high energy component. (The latter is an artifact caused by an electron beam being focused to a spot, causing reduction of the phosphate to phosphide - note also the lower O intensity. Such behaviour was not

found for the larger area  $\phi$ -phase as the electron beam was rastered, imparting a much lower electron dose).

Fe and Nd are present in the spectra of both phases. This is indicative of either a  $\text{Fe}_x\text{Nd}_{1-x}\text{PO}_4$  type compound (where  $x$  is larger for the  $\phi$ -phase matrix) or the presence of both the Fe and Nd phosphates. In either case, the important result is total coverage of the magnet by a protective phosphate layer. SEM/EDX results from the magnet phosphated in the alkaline solution (*solution 2*) are shown in Fig. 2.

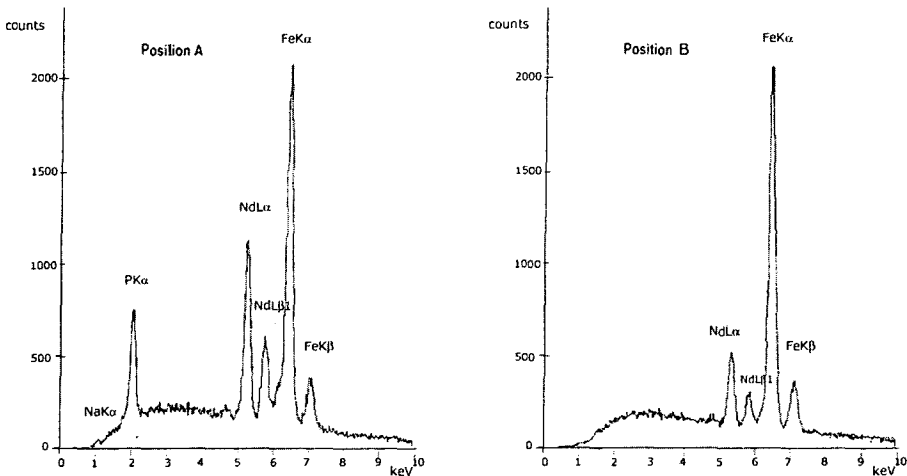
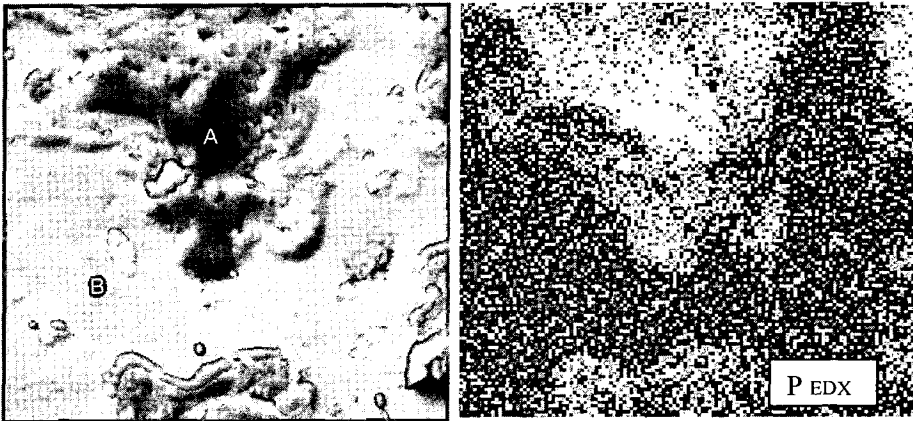


**Fig. 2.** (Upper) SEM micrograph and EDX P image of an incipient phosphated region formed in alkaline solution. (Lower) EDX point spectra from points A (left) and B (right) in SEM image.

These results indicate incipient phosphating and suggest how the process takes place. Comparison of the SEM image and P EDX map shows the non-uniform distribution of phosphate on the magnet surface. It is evident from the EDX spectrum of point B, that no phosphate has been deposited in this area and the phosphate layer formed on the magnet surface using the alkaline P solution is very

localised. The EDX spectrum taken from the deposit (point A) shows the phosphate to be Nd-rich compared to the matrix (point B). This may be related to porosity in the sintered magnet, since at pores, the magnet is more susceptible to corrosion.

It is likely that after the initial corrosion of the Nd-rich phase (more active than the matrix  $\phi$ -phase) leaching out Nd ions, prompt precipitation of Nd-phosphate occurs. The solubility product of Nd-phosphate is very low ( $K_{ps} \sim 10^{-28}$ ) [14] whereas that of ferric phosphate and ferrous phosphate are around  $10^{-20}$  and  $10^{-13}$ , respectively [15]. The corrosive attack of the magnet in alkaline solution is not favored and  $Fe^{2+}$  production is vital at the process startup to form the conversion coating layer and keep it growing. In alkaline solution, it is likely that the concentration of  $Fe^{2+}$  formed by corrosive attack is not sufficient to allow the formation of a continuous phosphate layer. In acid solutions, however, large  $Fe^{2+}$  concentrations are generated allowing the formation of a fairly continuous coating. This explains the dependence of the corrosion performance of the phosphate coating on the acidity of the phosphating solution.

After washing the phosphated magnet in an ultrasonic bath, AES analysis indicated that the phosphate layer had been removed from the surface. This observation provides further evidence that the precipitation of the phosphate formed in alkaline solution did not provide an adherent and protective layer.

Fig. 3 shows EIS results for phosphated and non-phosphated magnets, in  $Na_2SO_4$  electrolyte. The resistance of the conversion coating layer was estimated from the modulus of impedance at  $2 \times 10^{-2}$  Hz. The resistance obtained in acid solution was in the range of 5000 to 20000  $\Omega \text{ cm}^2$  whereas in alkaline solution it was less than 1000  $\Omega \text{ cm}^2$ . Phosphating in alkaline solution only increased the resistance of the magnet slightly, suggesting that the pH of the phosphating solution strongly affects the corrosion resistance.

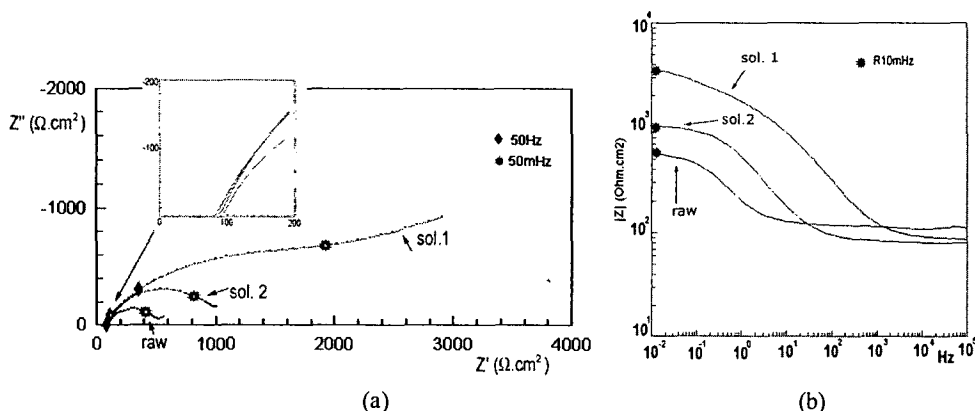


Fig. 3. EIS results of phosphated and untreated magnets in 0.01M  $Na_2SO_4$ . (a) Nyquist and (b) Bode plots. Phosphating: Sol. 1 (0.15 M  $NaH_2PO_4$ ; pH=4.6). Sol. 2 (0.15 M  $Na_2HPO_4$ ; pH=9.3).

Regarding the corrosion phenomena taking place on the untreated and phosphated magnets, examination of the diagrams presented in Fig. 3 shows that, for the untreated surface, only one time constant, linked to charge transfer processes at the magnet surface, is present. On the other hand, for the phosphated magnets, there is evidence of another time constant at higher frequencies. However, for phosphate coatings produced in solution 2, in the intermediate frequency range, this first loop is similar to that of the untreated magnet, indicating the existence of two highly

superimposed time constants, one at higher frequencies linked to the presence of a defective conversion layer, and the other, at lower frequencies, associated with charge transfer phenomena at the electrode surface.

For phosphated electrodes produced in solution 1, Fig. 3(a) shows the presence of a deformed high frequency capacitive loop followed by a low frequency capacitive loop. The first loop can be attributed to the presence of a porous homogeneous phosphate conversion layer and the second loop to charge transfer phenomena. The observation that the high frequency capacitive loop begins at higher frequency for electrodes produced in solution 1 (acidic) is further evidence of the better protective characteristics of conversion layers produced in acidic phosphating baths.

## Conclusions

The corrosion behavior of NdFeB phosphated and untreated magnets was investigated using EIS. The results showed that the corrosion resistance of NdFeB magnets can be improved by a conversion coating on top of the base material. However, the performance of this coating is strongly dependent on the pH of the phosphating solution, with acid baths producing much more protective coatings than alkaline baths. Auger analysis revealed the presence of phosphate on both phases ( $\varphi$ -phase and Nd-rich phase) of the magnet phosphated in the acid solution. Phosphating in alkaline solution resulted in localized precipitation of Nd-rich phosphates, discontinuity and lack of adherence of the conversion coating. The results indicated that phosphating of NdFeB magnets in alkaline medium is inadequate.

## References

- [1] R.H.J. Fastenau, van E.J. Loenen, *Journal of Magnetism and Magnetic Materials*, 157-158, (1996), p.1.
- [2] G.W. Warren, G. Gao, Q. Li, *Journal of Applied Physics*, 70 (10), (1991), p. 6609.
- [3] S. Hirosawa, S. Mino, H. Tomizawa, *Journal of Applied Physics*, 69 (8), (1991), p. 5844.
- [4] C.J. Willman, K.S.V.L. Narasimhan, *Journal of Applied Physics*, 61 (8), (1987), p. 3766.
- [5] K. Tokuhara, S. Hirosawa, *Journal of Applied Physics*, 69 (8), (1991), p. 5521.
- [6] H. Bala, G. Pawlowska, S. Szymura, V.V. Sergeev, Y. M. Rabinovich, *Journal of Magnetism and Magnetic Materials*, 87, (1990), p.L255.
- [7] H. Bala, G. Pawlowska, S. Szymura, Y. M. Rabinovich, *British Corrosion Journal*, 33 (1), (1998), p.37.
- [8] A.S. Kim, F.E. Camp, *Journal of Applied Physics*, 79 (8 part 2A), (1996), p. 5035.
- [9] C.W. Cheng, F.T. Cheng, *Journal of Applied Physics*, 83 (11), (1998), p. 6417.
- [10] C.D. Qin, A.S.K. Li, D.H.L. Ng, *J. of Appl. Physics*, 79 (8), (1996), p.4854.
- [11] F.H. Firsching, J.C. Kell, *J.Chem.Eng.Data*, 38, (1993), p. 132.
- [12] E. Pierri, D. Tsamouras, E. Dalas, *Journal of Crystal Growth*, 213, (2000), p. 93.
- [13] I. Costa, I.J. Sayeg, R.N. Faria, *IEEE Transactions on Magnetics*, 33 (5), (1997), p. 3907.
- [14] A.M. Saliba-Silva, I. Costa, *Key Engineering Materials*, 189-191, (2001), p. 363.
- [15] A.M. Saliba-Silva, M.A. Baker, M.A., H.G. de Melo, I. Costa, *Surface Treatment V, Series: Computational and Experimental Methods*, Ed. Brebbia, C.A., (2001), p. 65.
- [16] R.Franke, T. Chasse, P. Streubel, A. Meisel, *J. Electron Spectrosc. Relat. Phenom.* 56, (1991), p. 381.